Subdiffraction Light Focusing on a Grating Substrate

Anne Sentenac* and Patrick C. Chaumet

Institut Fresnel (UMR 6133), Université d'Aix-Marseille III, Avenue Escadrille Normandie-Niemen, F-13397 Marseille cedex 20, France

(Received 18 December 2007; revised manuscript received 17 May 2008; published 30 June 2008)

We describe a way to generate subdiffraction light spots that can be moved over a surface without resorting to near-field manipulation, nonlinear effects, or negative index materials. We use a periodically patterned substrate that converted efficiently, through scattering, the impinging propagative waves into evanescent ones. Then we optimize the wave front of the incident propagative beam so that the grating-scattered evanescent waves interfere constructively at the focal point. Numerical simulations show that focus spots as small as one-sixth of a wavelength can be obtained at any point on the substrate. One foreseen application is high resolution surface imaging.

DOI: 10.1103/PhysRevLett.101.013901 PACS numbers: 42.30.−d, 42.25.−p

The problem of focusing light beams into small volumes has received considerable attention in the past decade as it finds applications in many different fields such as high resolution imaging [1], optical lithography [2], optical data storage [3], or particle trapping [4]. In conventional optics, the spot size is essentially limited to half the wavelength since the field Fourier components with spatial frequencies greater than the free-space wave number $k_0 = 2\pi/\lambda$ cannot propagate. Subwavelength focusing requires the presence of high spatial frequency evanescent waves which are usually generated by drawing an object in the near field of the focal point, like a sharp tip or a tapered optical fiber as in near-field optical microscopy [5]. The main drawback of this technique is that moving the light spot requires the displacement of the near-field object in the subwavelength proximity of the sample. To avoid this near-field manipulation, it has been proposed to enhance the weight of the evanescent waves that contribute to the subwavelength focusing using nonlinear effects [6], a negative refraction superlens [7], or a combination of the two [8]. However, these techniques necessitate high power lasers or sophisticated metamaterials [9,10].

In this work, we propose a new approach to create subdiffraction light spots which can be manipulated from the far field to scan a surface. The main idea was to use subwavelength gratings to convert, in a controlled way and throughout its surface, low spatial frequency incident propagative waves into high spatial frequency evanescent waves. The second idea was to optimize the wave front of the incident beam in order to build constructive interferences from the grating-scattered evanescent waves at any position on the grating surface. As discussed below, one important foreseen application of this approach is high resolution microscopy devoted to surface imaging [11].

The first step was to design the grating substrate that generates the high spatial frequency waves. Let us consider a two-dimensional grating that is illuminated from below by a monochromatic plane wave with frequency ω and wave vector $\mathbf{k}^{\text{inc}} = (\mathbf{k}_{\parallel}^{\text{inc}}, k_z^{\text{inc}})$, where the subscript $\parallel$ indicates the projection onto the plane of the substrate while the subscript z indicates the projection onto the normal of the substrate plane. Hereafter, the dependence in $\exp(-i\omega t)$ is omitted. The field just above the grating can be written as [12]

$$\mathbf{E}_{\text{ref}}(\mathbf{k}_{\parallel}^{\text{inc}}, \mathbf{r}_{\parallel}, z = 0) = \sum_{\mathbf{K}\in W} \mathbf{E}_{\mathbf{K}}(\mathbf{k}_{\parallel}^{\text{inc}}) e^{i(\mathbf{K}+\mathbf{k}_{\parallel}^{\text{inc}}).\mathbf{r}_{\parallel}}, \quad (1)$$

where W denotes the reciprocal space of the periodic structure. To obtain a subdiffraction spot, one needs to build a constructive interference pattern with waves presenting high spatial frequencies. One could illuminate the grating under several incident angles and fix the incident complex amplitudes so that, at the chosen focus point, the phase of one specific high spatial frequency term in Eq. (1) is the same whatever the incident angles. Unfortunately, the subdiffraction spot obtained with this partial constructive interference process is, in general, blurred by the contribution of all of the other terms. Thus, to facilitate the building of the subdiffraction spot, it is preferable that the series in Eq. (1) be reduced to only one Fourier coefficient [13,14], namely,

$$\mathbf{E}_{\text{ref}}(\mathbf{k}_{\parallel}^{\text{inc}}, \mathbf{r}_{\parallel}, z = 0) \approx \mathbf{E}_{\mathbf{K}_c}(\mathbf{k}_{\parallel}^{\text{inc}}) e^{i(\mathbf{K}_c+\mathbf{k}_{\parallel}^{\text{inc}}).\mathbf{r}_{\parallel}} \quad (2)$$

with the highest K_c possible. This property can be obtained, for certain incidences, with specially designed gratings called "resonant gratings." These structures are basically composed of a dielectric or metallo-dielectric multilayer harboring a periodic structuration. The incident wave is scattered into a mode of the multilayer, either a guided wave [15] or a surface plasmon [13,14] if the phase-matching condition [12]

$$k_p \approx |\mathbf{k}_{\parallel}^{\text{inc}} + \mathbf{K}_c| \quad (3)$$

is satisfied. In Eq. (3), k_p is the wave number of the mode and $\mathbf{K}_c \in W$ is the grating reciprocal space vector involved in the scattering process. The resonance phenomenon increases the amplitude of the corresponding field

component $\mathbf{E}_{\mathbf{K}_c}$ in Eq. (1). The main issue is then to design a structure that supports modes with high spatial frequency. In the UV domain, thin metallic films supporting surface plasmons can be used [13,14,16]. In the visible or infrared domains, dielectric slabs with high refractive index supporting guided modes can be more appropriate. In this work we considered a silicon slab with refractive index $n_a = 3.72 + i0.011$ at $\lambda = 700$ nm. Note that, at this wavelength, silicon is lossy and cannot be used to fabricate solid-immersion lenses. On the other hand, silicon slabs support lossy guided waves that can be excited with an adequate periodic structuration. We have optimized the resonant grating with rigorous calculations performed with a Fourier modal method [17]. The designed structure consists of a slab of Ta_2O_5 ($n_b = 2.1$) pierced by an hexagonal array of holes filled with silicon, sandwiched between two layers of silicon, and deposited on a glass prism ($n_s = 1.5$); see Fig. 1(a) for the geometrical dimensions. The homogenized multilayer supports a TM lossy guided wave with wave number k_p close to $3k_0$ at $\lambda = 700$ nm. The grating period is much smaller than the incident wavelength $d = 0.26\lambda$. Thanks to the $C6$ symmetry of the structure, the guided wave can be excited with six p-polarized incident plane waves (the electric field belongs to the incident plane) with azimuthal angles $\phi = n\pi/3$, $n = 1, \ldots, 6$, and equal polar angle $\theta_0 = 64°$ that ensures that the phase-matching condition Eq. (3) is satisfied. Under these conditions, the field above the grating is dominated by $\mathbf{E}_{\mathbf{K}_c}$, where $K_c = \frac{2\pi}{d}\frac{2}{\sqrt{3}}$. Outside these conditions, the grating behaves as a standard homogeneous multilayer, and the zero order in Eq. (1) is dominant.

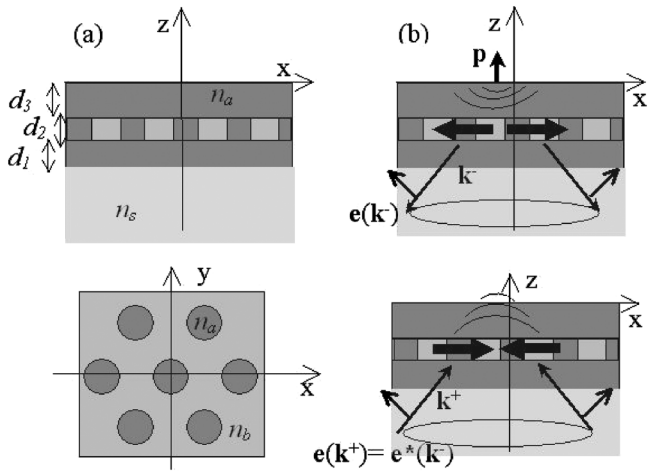

FIG. 1. (a) Geometry of the grating substrate. Side view (top) and top view (bottom): A slab of Ta_2O_5 ($n_b = 2.1$) is pierced by an hexagonal array of holes of period $d = 0.26\lambda$ filled with silicon ($n_a = 3.72 + i0.012$), sandwiched between two layers of silicon and deposited on a glass prism ($n_s = 1.5$). Radius of the holes: $r = 0.13\lambda$; layer thicknesses: $d_1 = 0.09\lambda$, $d_2 = 0.07\lambda$, and $d_3 = 0.18\lambda$, $\lambda = 700$ nm. (b) Principle of the phase conjugation focusing method (see text).

The second step was to define the phase and amplitude of the plane waves forming the incident beam in order to focus at a given point $\mathbf{r}$ on a substrate that is not translationally invariant. The simplest solution consists in using the phase conjugation or time-reversal focusing method, schematically depicted in Fig. 1(b). This approach consists in detecting the field radiated by an emitter placed at the chosen focus point and sending it back in time-reverse order (or with a phase conjugation for monochromatic fields) [18,19]. When the emitter is plunged into a random scattering medium, the time-reversed field can focus well below the diffraction limit [20] because of the conversion, through multiple scattering, of the incident propagative waves into evanescent ones. Thus, to generate a focus spot centered at $\mathbf{r}$ above the grating, we first calculated the complex amplitude $\mathbf{e}(\mathbf{k}^-)$ of the field diffracted in the $\mathbf{k}^- = (\mathbf{k}_\parallel, -k_z)$ direction, by a dipole $\mathbf{p}$ placed at $\mathbf{r}$ just above the grating [21] [see Fig. 1(b), top view]. Then we formed an incident beam composed of plane waves with wave vector $\mathbf{k}^+ = (\mathbf{k}_\parallel, k_z)$ and complex polarization taken equal to the complex conjugate of $\mathbf{e}(\mathbf{k}^-)$. One easily sees, by invoking the reciprocity theorem [22], that when the grating is illuminated by one incident plane wave satisfying this condition, the field amplitude at $\mathbf{r}$, projected on $\mathbf{p}$, is always real and positive. Thus, at least along the $\mathbf{p}$ direction, all of the fields induced by the different incident plane waves interfere constructively at $\mathbf{r}$ [Fig. 1(b), down view]. Note that this constructive interference process is not sufficient, in general, to ensure that the resulting field is maximum at the focus point over a given investigation domain. It is also required that the field modulus obtained separately for each incident angle be roughly constant over the investigation domain and that its component along $\mathbf{p}$ be dominant. These conditions can be satisfied with most resonant gratings at and outside the resonance Eqs. (2) and (3).

In our configuration, one wants to maximize the conversion role of the grating Eq. (2). Thus, only incident beams built from p-polarized plane waves with fixed polar angle θ_0 are considered. For such incident plane waves, the z component of the transmitted field above the grating is predominant. Hence, to specify the complex amplitude of the plane waves forming the incident beam with the phase conjugation method, we chose a dipole oriented along the z axis and simulated its p-polarized diffracted far field along a circular cone with half-angle $\theta = 64°$. Note that, the high frequency Fourier components of the grating field decaying exponentially as one moves away from the grating, Eq. (2) is valid only in the close vicinity of the grating. Hence, the dipole is placed at $z = 0$, and the subdiffraction spots are necessarily bound to the grating surface.

We first studied the focal spot created by this approach when the substrate is a glass substrate covered by a silicon layer [the periodical structuration has been removed; see Fig. 2(a)]. The substrate is illuminated with 24 p-polarized

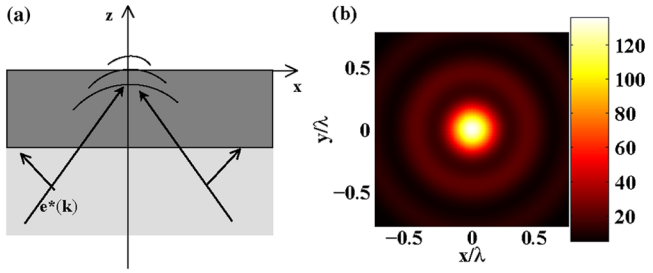

FIG. 2 (color online). Light focusing on a homogeneous prism covered by a silicon layer. (a) Geometry. (b) Intensity map obtained at $z = 0$ nm when the substrate is illuminated with 24 p-polarized plane waves, with polar angle equal to $\theta_0 = 64°$ and azimuthal angles $\phi = q\pi/12$, where $q = 1, \ldots, 24$.

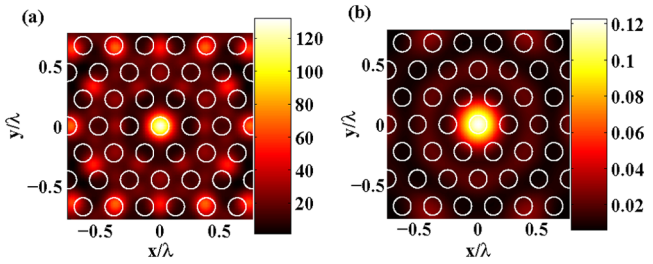

FIG. 3 (color online). Light focusing on the grating substrate depicted in Fig. 1 using an incident beam specified with the phase conjugation method described in Fig. 2. (a) Intensity at $z = 0$. (b) Intensity at $z = \lambda/2$.

plane waves, with polar angle equal to θ_0 and azimuthal angles $\phi = q\pi/12$, where $q = 1, \ldots, 24$. Their complex amplitudes are fixed with the phase conjugation technique by placing the dipole at the phase origin $\mathbf{r} = 0$. Because of the radial symmetry of this configuration, the complex amplitudes of all of the incident plane waves are equal. The constructed incident beam resembles a radially polarized Bessel beam, except that it is not made of an infinite number of plane waves. Now, Bessel beams have been shown to yield very small transverse focal spots [2,23]. In our configuration, the incident plane waves are totally reflected at the prism-air interface, so that the beam is evanescent in air. Its intensity decays exponentially as one moves away from the interface, but its transverse intensity pattern remains unchanged. One can approximate the field intensity about the focal point by $I(r_\parallel, z) \approx \exp(-2k_z z)|J_0(k_\parallel r_\parallel)|^2$, where $k_\parallel = n_s k_0 \sin\theta_0$ and $k_z = \sqrt{k_\parallel^2 - k_0^2}$. The simulated field intensity map at $z = 0$ plotted in Fig. 2(b) is in agreement with this analytical expression. The width at half maximum of the focal spot is about 0.3λ, which is already a marked improvement on the standard focal dimensions obtained with classical strongly focused Gaussian beams [2,23].

We now replace the homogeneous substrate by the periodically structured substrate. We first create an incident beam that focuses at the phase origin $\mathbf{r} = 0$, which happens to be a symmetry point of the grating (it is located above the center of one silicon rod of the hexagonal array). The beam is composed of 24 p-polarized plane waves with the same polar and azimuthal angles as described above. Because of the $C6$ symmetry of this configuration, the amplitudes of the incident waves that can be deduced from one another by a $\pi/3$ rotation about the z axis are found to be equal. When they do not satisfy this condition, their amplitude differ in modulus and phase. More precisely, the modulus of the six incident waves with azimuthal angle $\phi = n\pi/3$, $n = 1, \ldots, 6$, that couple efficiently to the TM guided mode is found to be 3 times as big as that of the 18 other waves. We plot in Fig. 3(a) the field intensity map obtained at $z = 0$ when the grating is illuminated by this optimized beam. We observe an intense focus spot of full width at half maximum close to $\lambda/6$ at $\mathbf{r} = 0$. Thus, by using a patterned substrate it is possible to divide the width of the focal spot by a factor close to 2. This achievement is brought about by the efficient conversion into high spatial frequency guided waves of the six incident plane waves that verify the phase-matching condition. The interference pattern of the six guided waves is basically a strongly undersampled Bessel beam with an argument close to $k_p r_\parallel$. It is responsible for the subdiffraction width of the focal spot and the marked secondary maxima observed in Fig. 3(a). The 18 other plane waves do not contribute to the subdiffraction focusing. Their role is to reduce the strength of the secondary maxima in the vicinity of the focal region. Figure 3(b) shows the intensity map of the field at an altitude of $\lambda/2$ above the grating. As expected, the secondary maxima have disappeared, confirming their strong evanescent nature, and the beam intensity repartition is now similar to that of the Bessel beam obtained in the homogeneous case (Fig. 2).

Figure 3(a) shows that our approach permits us to generate a subdiffraction light spot above a silicon rod of a periodically patterned substrate. Now, a similar result could be easily obtained by illuminating a metallic slab pierced with subwavelength holes or a structured dielectric mask as in advanced contact lithography techniques. However, in these examples, the location of the light spot is determined by the topography of the mask. The spot appears above the protrusion of the dielectric substrate [24], above the hole of the metallic layer, or at the antinodes of a fixed plasmon stationnary wave [16]. It cannot be moved to scan a surface (except by moving the mask). In contrast, the main interest of our approach is that the light spot can be formed at any point on the grating by changing the wave front of the incident beam. To illustrate this critical assertion, we plot in Fig. 4(a) the intensity map at $z = 0$ obtained when the grating is illuminated by an incident beam that is optimized to focus at equidistance between two silicon rods, i.e., above the low refractive index region of the grating. The beam is composed of 24 plane waves whose complex amplitudes have been specified by simulating the field diffracted by a

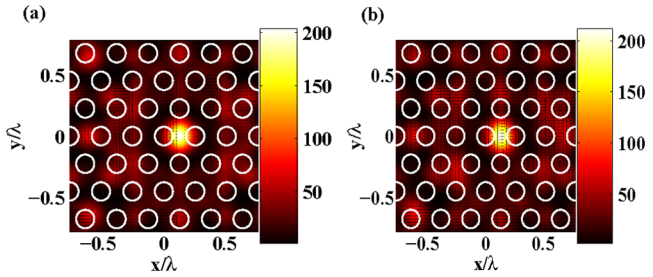

FIG. 4 (color online). (a) As in Fig. 3(a) except that the focus spot is located at an equidistance between two holes. (b) As in (a) except that the complex amplitudes of the 24 incident plane waves are perturbed by a random Gaussian noise on both the real and the imaginary parts.

z-polarized dipole at ($z = 0$, $x = d/2$, $y = 0$). We observe that the shape of the focal spot remains very close to that obtained at a symmetry point. We have checked, with other simulations, that the focal spot could be moved continuously on the substrate without significant distortion just by changing the phase and amplitudes of the impinging plane waves.

For practical applications, it was also necessary to verify that focusing is not too sensitive to errors on the relative phases and moduli of the different incident plane waves forming the incident beam. The complex amplitudes of the 24 incident plane waves used in Fig. 3 were perturbed by a random Gaussian noise on both the real and the imaginary parts. The noise variance was taken equal to 10% of the maximum of the moduli. With such a noise, the phase difference between the perturbed and exact amplitude may reach 40°. Figure 4(b) shows the intensity map obtained at $z = 0$ when the grating is illuminated by the perturbed incident beam. We note that the focal spot was not significantly modified as compared to Fig. 4(a). Indeed, the phase conjugation focusing technique is very robust to noise.

In conclusion, we show that, by illuminating a subwavelength resonant grating with an optimized propagating beam, it is possible to generate a subdiffraction light spot at any point on the substrate. The spot width d depends on the grating ability to convert an incident wave with low spatial frequency $k_{\|}^{\mathrm{inc}}$ into an evanescent wave with high spatial frequency k_p, $d \approx \pi/k_p$. In this work, we obtained a spot width about $\lambda/6$ at $\lambda = 700$ nm with a resonant silicon grating supporting a guided mode with $k_p \approx 3k_0$. A resolution better than $\lambda/10$ could be expected with gratings supporting higher spatial frequency modes like the surface plasmons modes exhibited in the UV domain in thin metallic films [16]. One potential application of our setup is optical surface microscopy. In this case, the sample would be deposited on the grating substrate and introduced in a microscope that would admit complex illumination schemes. By controlling dynamically the wave front of the incident beam, for example, with a spatial light modulator [4], it would be possible to generate and move a subdiffraction spot at the grating surface in order to scan the sample at high resolution. The same setup could be used to manipulate selectively nanoparticles on the substrate [4,25].

The authors thank P. Balse and A.-G. Sentenac for a careful reading of the manuscript.

*anne.sentenac@fresnel.fr

[1] S. Hell, Science **316**, 1153 (2007).
[2] T. Grosjean, D. Courjon, and C. Bainier, Opt. Lett. **32**, 976 (2007).
[3] A. S. van de Nes, J. J. M. Braat, and S. F. Pereira, Rep. Prog. Phys. **69**, 2323 (2006).
[4] D. G. Grier, Nature (London) **424**, 810 (2003).
[5] R. Hillenbrandt, T. Taubner, and F. Keilmann, Nature (London) **418**, 159 (2002).
[6] J. Wei, M. Xiao, and F. Zhang, Appl. Phys. Lett. **89**, 223126 (2006).
[7] J. Pendry, Phys. Rev. Lett. **85**, 3966 (2000).
[8] A. Husakou and B. Hermann, Phys. Rev. Lett. **96**, 013902 (2006).
[9] R. A. Shelby, D. R. Smith, and S. Schultz, Science **292**, 77 (2001).
[10] E. Cubukcu, K. Aydin, E. Ozbay, S. Foteinopoulou, and C. M. Soukoulis, Nature (London) **423**, 604 (2003).
[11] J. K. Jaiswal and S. M. Simon, Nature Chem. Biol. **3**, 92 (2007).
[12] R. Petit, *Electromagnetic Theory of Gratings* (Springer-Verlag, Berlin, 1980).
[13] A. Sentenac, P. C. Chaumet, and K. Belkebir, Phys. Rev. Lett. **97**, 243901 (2006).
[14] Z. Liu, S. Durant, H. Lee, Y. Pikus, N. Fang, Y. Xiong, C. Sun, and X. Zhang, Nano Lett. **7**, 403 (2007).
[15] A. L. Fehrembach, D. Maystre, and A. Sentenac, J. Opt. Soc. Am. A **19**, 1136 (2002).
[16] X. Luo and T. Hishihara, Opt. Express **12**, 3055 (2004).
[17] L. Li, J. Opt. Soc. Am. A **14**, 2758 (1997).
[18] M. Fink, Phys. Today **50**, No. 3, 34 (1997).
[19] R. Carminati, R. Pierrat, J. de Rosny, and M. Fink, Opt. Lett. **32**, 3107 (2007).
[20] G. Lerosey, J. de Rosny, and M. Fink, Science **315**, 1120 (2007).
[21] A. L. Fehrembach, S. Enoch, and A. Sentenac, Appl. Phys. Lett. **79**, 4280 (2001).
[22] J.-J. Greffet and R. Carminati, Prog. Surf. Sci. **56**, 133 (1997).
[23] R. Dorn, S. Quabis, and G. Leuchs, Phys. Rev. Lett. **91**, 233901 (2003).
[24] O. J. F. Martin, Microelectron. Eng. **67–68**, 24 (2003).
[25] P. C. Chaumet, A. Rahmani, and M. Nieto-Vesperinas, Phys. Rev. B **66**, 195405 (2002).